

A.M.S. Richards¹, Y. Asaki², A. Baudry³, J. Brand⁴, F. Cowie¹, L. Decin⁵, S. Etoka¹, M.D. Gray⁶, F. Herpin³, R. Humphreys⁷, B. Pimpanuwat¹, A. Singh⁸, J.A. Yates⁹, L. Ziurys⁸
¹JBCA, U. Manchester, UK; ²JAO, Chile, SOKENDAI, Japan; ³LAB, CNRS, France; ⁴INAF, Italy; ⁵KU Leuven, Belgium; ⁶NARIT, Thailand; ⁷U. Minnesota, USA; ⁸U. Arizona, USA; ⁹UCL, UK

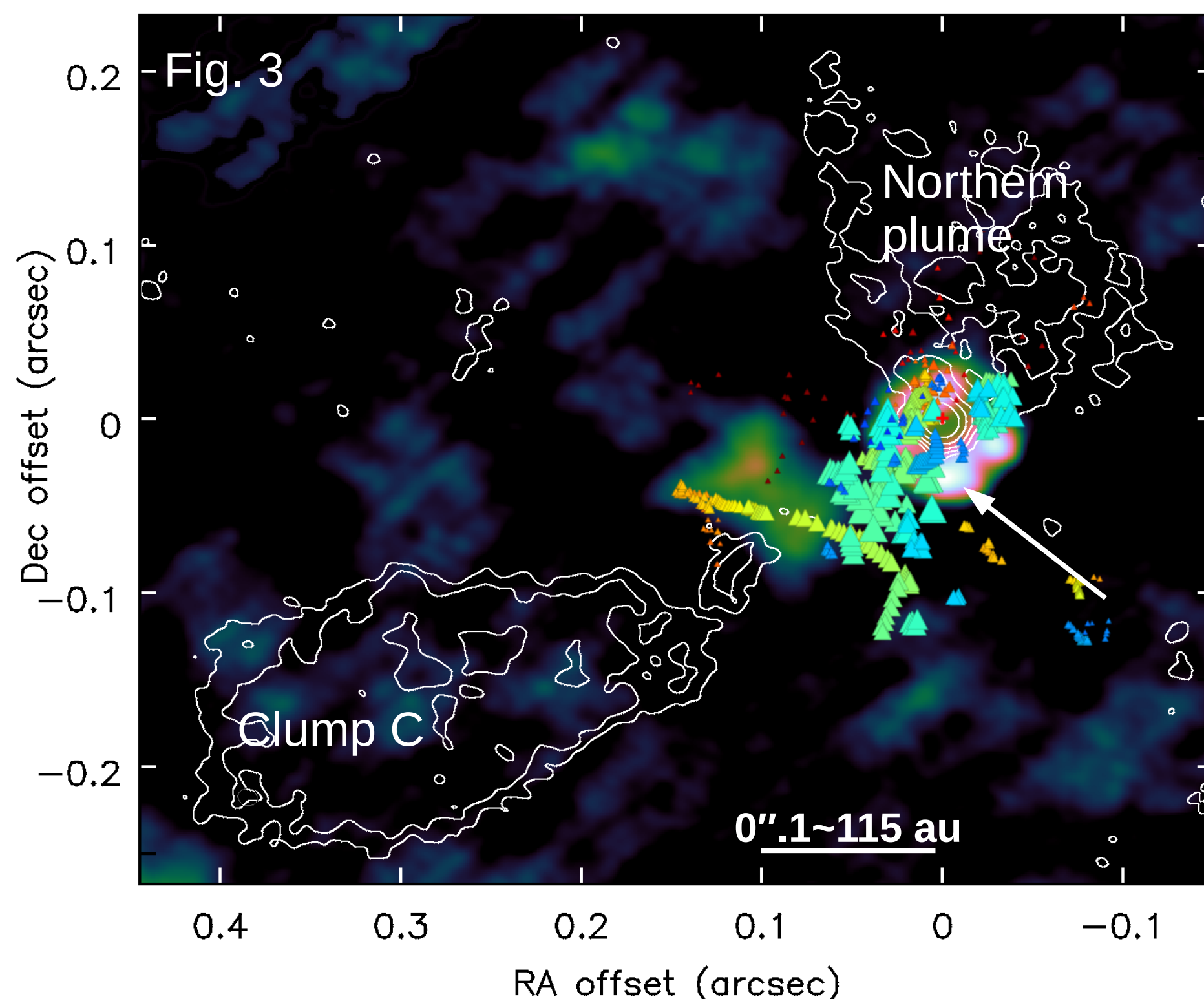
Comparing water maser models and observations around VY CMA

- Reconstruct local variations in physical conditions on the scales of clumps;
- Trace clumps, shocks, asymmetry, ejecta, the background wind;
- Constrain models

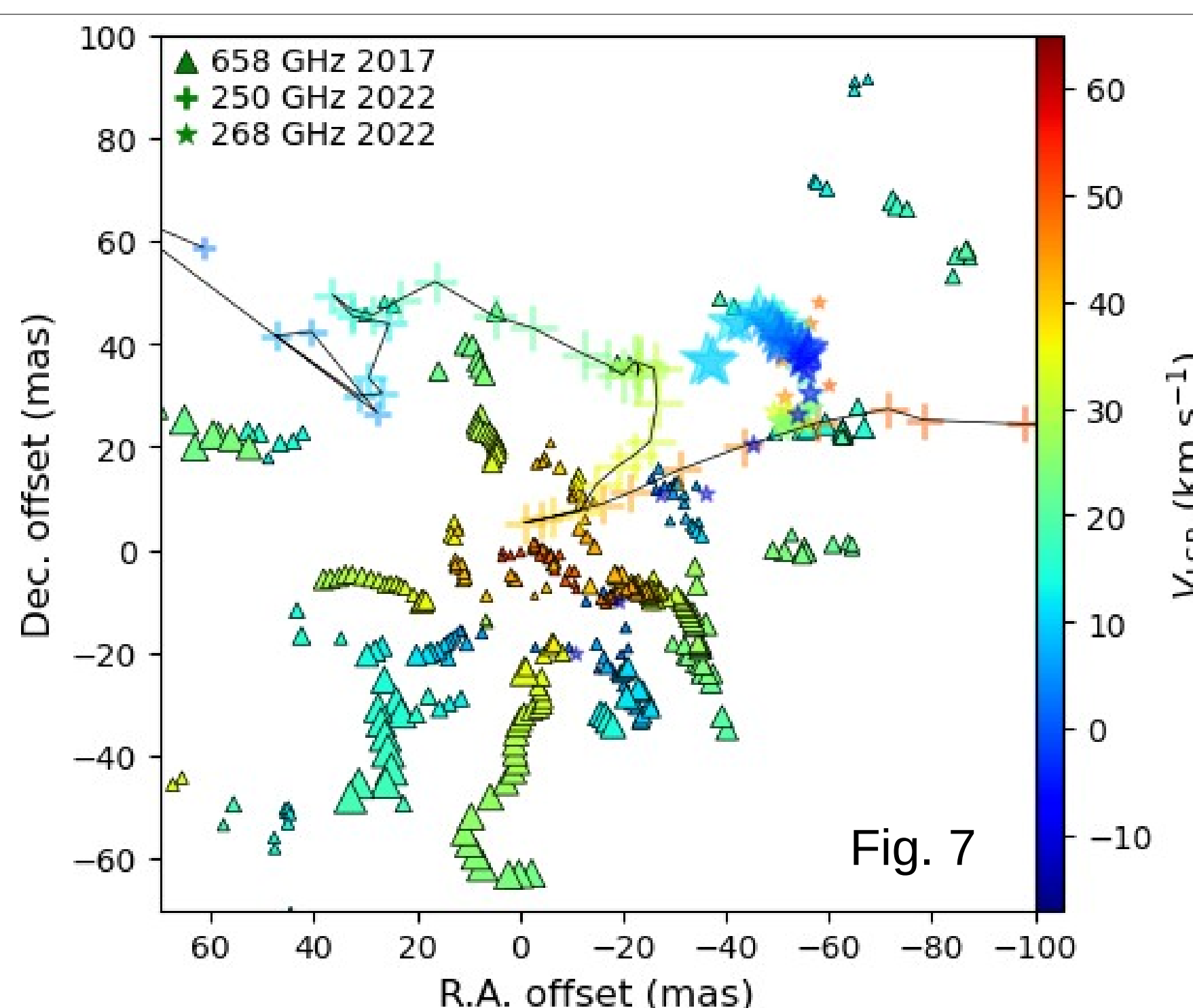
Maser amplification allows imaging at an order of magnitude higher resolution (spatial and spectral) than thermal lines. Distinctive, persistent position-velocity patterns show that series of maser spots following a position-velocity gradient can trace discrete physical clumps (Richards et al. 2012). Water masers at cm to sub-mm wavelengths have excitation temperatures from ~200 – 7000 K. Each line emanates from a characteristic range of gas and dust temperatures, number densities, radiation fields, abundances and so on. Applying models (Gray et al. 2016) to local overlap or avoidance of different maser transitions allow us to map these physical conditions. Variability can be related to changes in irradiation or shocks (Gray et al. 2020; 2023 in prep.).

Dust clumps, 658 GHz masers and KI knot

Fig. 3 white contours show continuum emission from dust and the star, at (0,0). The background colours show 658 GHz maser intensity at 30–34 km/s observed in 2017 (Asaki et al. 2020). They form a ring consistent with tangential beaming from an accelerating shell, with a diffuse arc towards C. 658 GHz maser spot positions mapped in 2013 are overlaid, colour coded as in Fig. 1. Only the E of the ring is seen but the arc is better defined. All masers (and thermal lines) avoid C. Its spectral index suggests it contains >1e-3 M_⊙ dust, cold and optically thick (Vlemmings et al. 2017).

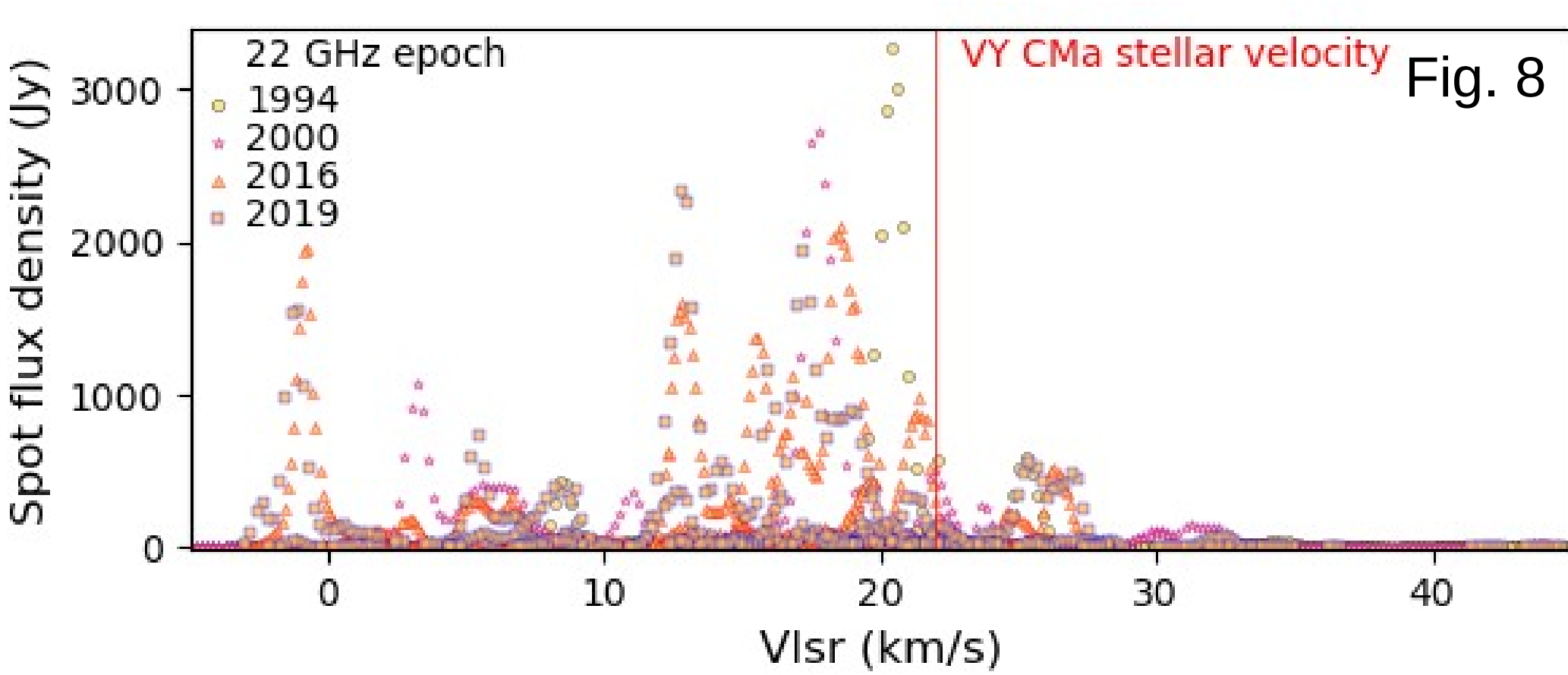


The arrow marks the position of one of the knots of KI emission (HST, Humphreys et al. 2021), ejected from the star in recent decades, which reached conditions for 658 GHz masing (Fig. 4) since 2013.



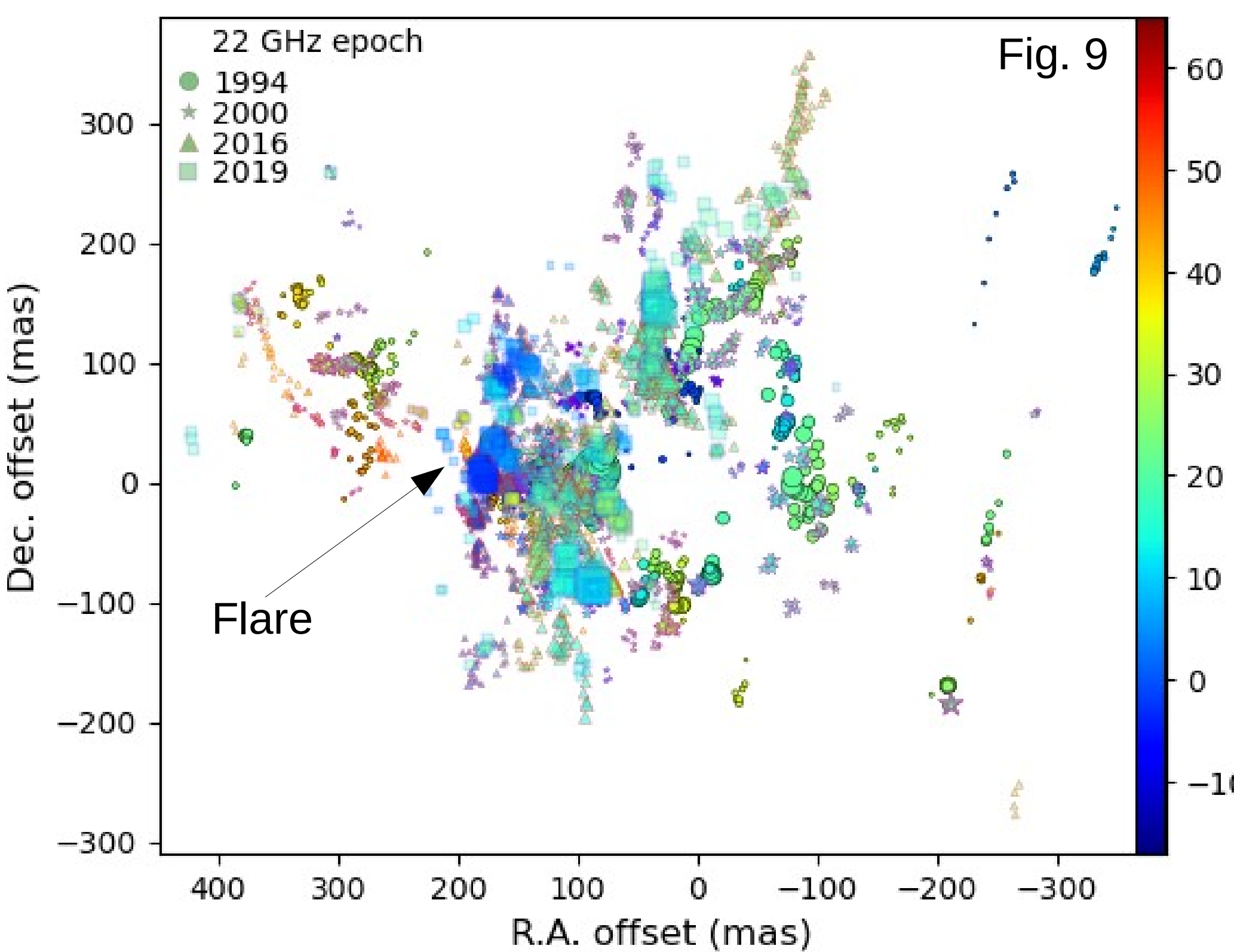
Dynamic inner 10 R_{*}

A slice through the hollow shell of 658 GHz emission is seen in Fig. 3. Fig. 7 shows radial streams of maser spots, with T_b up to 3e6 K. The 250 and 268 GHz lines were observed at lower angular resolution, with $T_b > 500$ K and 5e5 K, respectively. The latter is masing, confined to an NW arc; the requirement for high T_{dust} (Fig. 4) suggests a shock. Some 250-GHz emission may be thermal but the arc (joined by a line) could trace the same outflow.



Shock diagnostics?

22 GHz masers extend from -10 to 50 km/s. Up to 2000, emission over a few 100 Jy occurred within 10 km/s of V_* , but a new peak is seen in Fig. 8 around -1 km/s in 2016 and 2019. Fig. 9 shows the flare location, in the direction of clump C. The brightening material extends ~100 mas, suggesting a shock front rather than local cloud overlap. The 183-GHz emission observed in 2017 has a peak at a similar velocity and location, suggesting $n \sim 1e15$ m⁻³, $T \sim 1000$ K. The SW part of the shell has, however, faded.

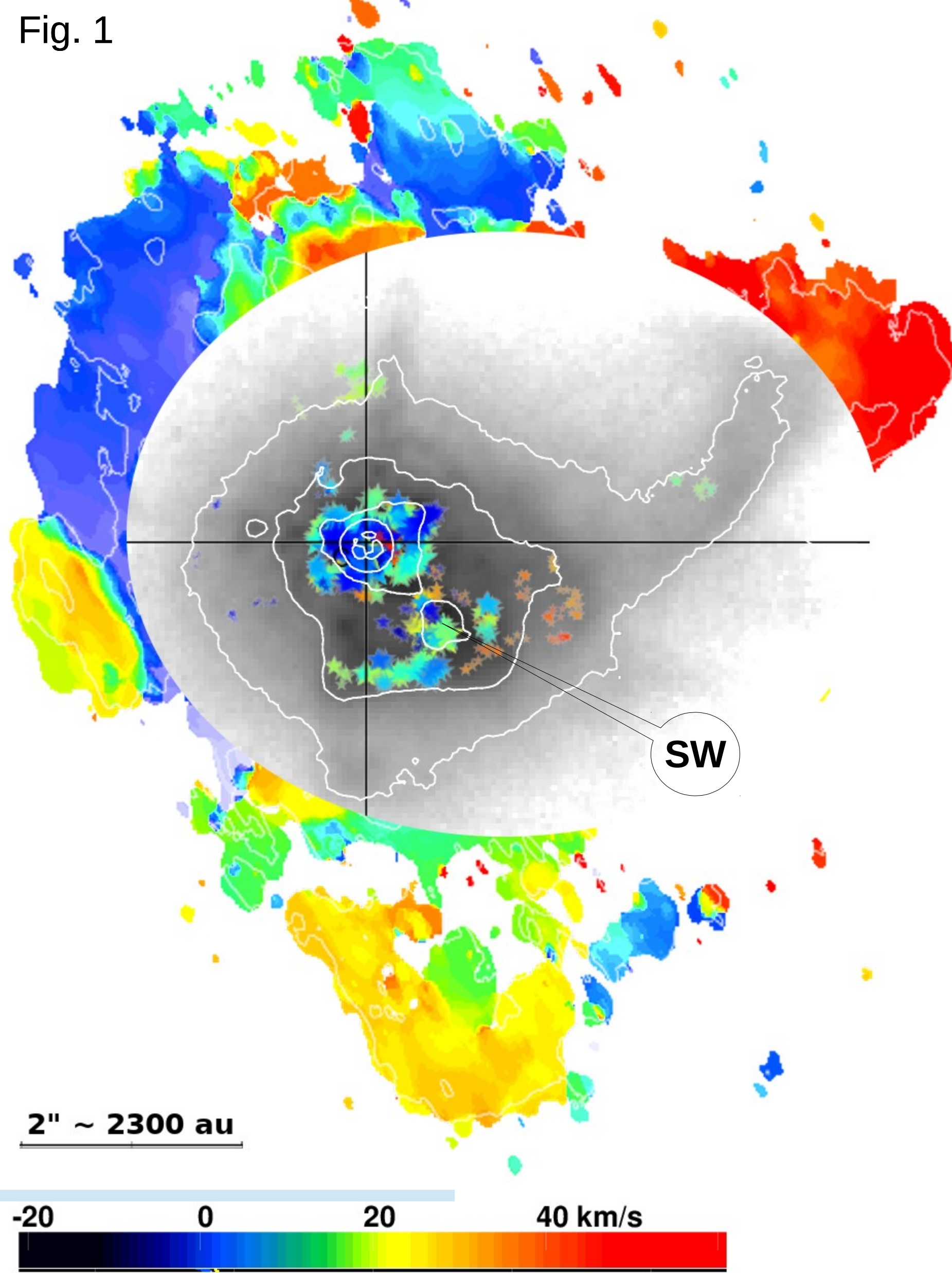


References

Asaki et al. 2020, ApJS, 247, 33
 Choi et al. 2008, PASJ, 60, 1007
 Decin et al. 2006 A&A, 456, 549
 Gray et al. 2016, MNRAS, 456, 374
 Gray et al. 2020, MNRAS, 493, 2472
 Humphreys et al. 2021, AJ, 161, 98
 Richards et al. 2012, A&A, 546, A16
 Richards et al. 2014, A&A, 572, L9
 Smith et al. 2001, AJ, 121, 1111
 Wittkowski et al. 2012, A&A, 540, L12
 Vlemmings et al., 2017, A&A, 603, A92
 Zhang et al. 2012, ApJ, 744, 23

This poster uses data from ALMA, e-MERLIN and HST, and DiRAC and IRIS computing facilities.

Fig. 1

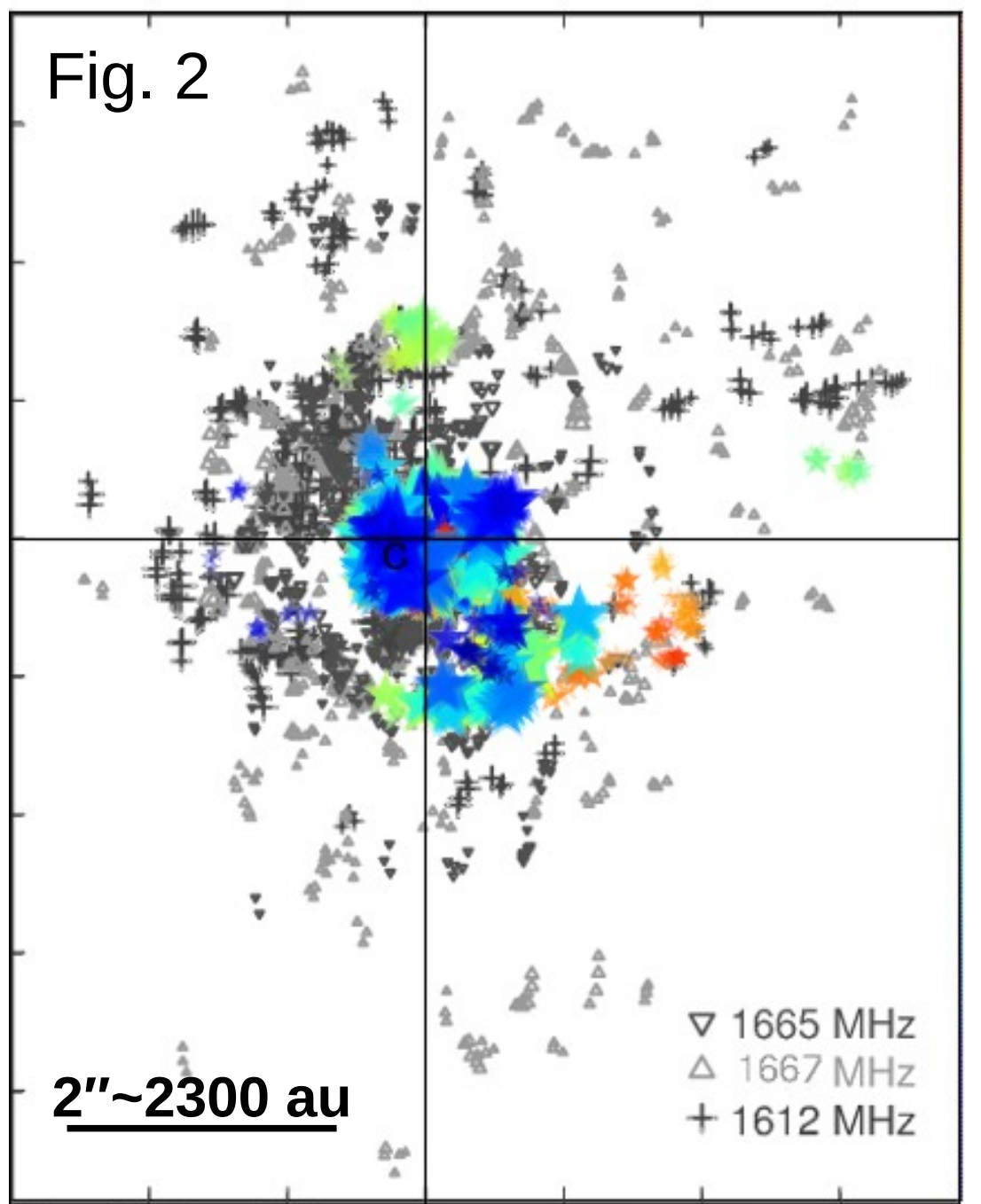


Red Supergiant VY CMA

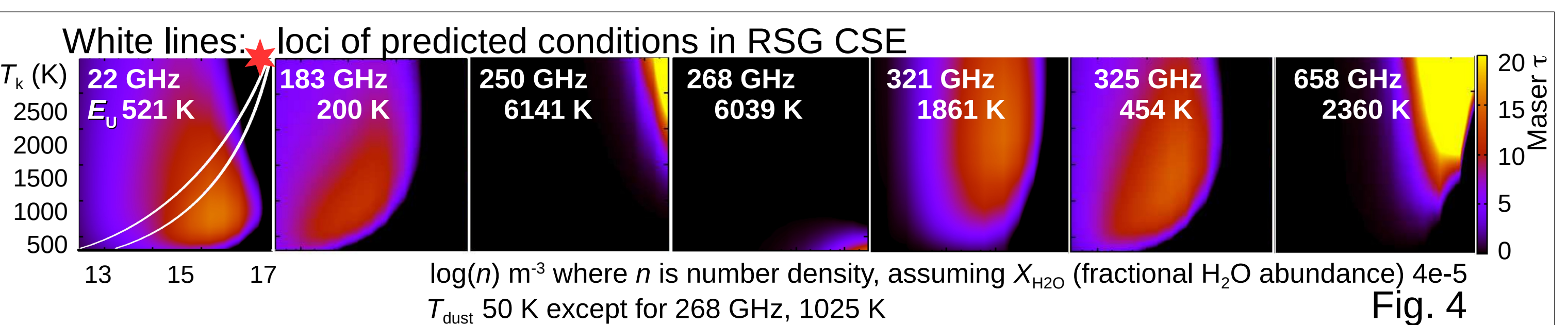
D~1,15 kpc (Choi et al. 2008; Zhang et al. 2012); R_* 5.7 mas (Wittkowski et al. 2012); \dot{M} 5e-5 – 1e-3 M_⊙/yr (Decin et al. 2006).

The big picture

Fig. 1 shows velocity-weighted intensity ALMA observations of SO₂ in the background. The star is at the axes intersection. The inset greyscale and white contours show light scattered by small dust grains (HST, Smith et al. 2001). Velocity-colour-coded positions of 183-GHz maser components (ALMA) are overlaid. OH masers are shown below in Fig. 2, star at (0,0).



OH 1665/7 MHz masers overlap the outer 22-GHz H₂O maser shell, suggesting cooler, less dense gas ($T < 500$ K, $n < 5e11$ m⁻³) surrounding the 22-GHz clumps. OH masers reach further from the star than all water transitions but are weaker to the SW where 183 GHz masers are extended. The latter tolerate warmer conditions and hotter dust radiation. 250-GHz (quasi-)thermal H₂O emission is also extended SW.



Maser modelling

We use Gray et al. (2016) (Fig. 4) to infer the conditions in the wind supporting various combinations of masers, for 321, 325 and 658 GHz masers observed in 2013 and the 183 GHz masers, assuming collisional pumping. Maps (Richards et al. 2014) show that lines with lower E_U indeed peak at greater distances from the star. Fig. 5 shows where the lines are expected to overlap or segregate.

The inferences are compared with models for the wind of VY CMA derived by Decin et al. (2006) from Herschel data in Fig. 6. 22-GHz masers were previously thought to come from dense clumps (Richards et al. 2012). VY CMA's X_{H_2O} may vary and is probably $> 3e-5$; maser τ has a log dependence on X_{H_2O} , which could reduce overdensity to a factor of ~20-30. Using a gradient in T_{dust} as well as T_k will extend the ranges of some lines e.g. 321 GHz and reduce others. Some lines e.g. 268 GHz are radiatively pumped by hot dust.

